

Magnetic susceptibility and low-temperature structure of the linear chain cuprate Sr_2CuO_3

T. Ami,* M. K. Crawford, and R. L. Harlow
Du Pont, Wilmington, Delaware 19880-0356

Z. R. Wang and D. C. Johnston
Ames Laboratory and Department of Physics and Astronomy, Iowa State University, Ames, Iowa 50011

Q. Huang
*National Institute of Standards and Technology, Bldg. 235, Gaithersburg, Maryland 20899
 and Department of Materials and Nuclear Engineering, University of Maryland, College Park, Maryland 20742*

R. W. Erwin
*National Institute of Standards and Technology, Bldg. 235, Gaithersburg, Maryland 20899
 (Received 24 March 1994; revised manuscript received 20 September 1994)*

Magnetic susceptibility measurements for $\text{Sr}_2\text{CuO}_{3\pm\delta}$ were made from 2 to 800 K, and a strong dependence upon oxygen content (δ) was observed. Samples synthesized under oxygen, followed by various nitrogen treatments, exhibited markedly different Curie-Weiss-type terms, and we discuss possible origins for this behavior. High-temperature magnetic susceptibility measurements for the sample with the smallest Curie-Weiss-type term clearly show the increase with temperature expected from the Bonner-Fisher model for a spin- $\frac{1}{2}$ one-dimensional (1D) Heisenberg antiferromagnet. This is a direct experimental observation of 1D magnetic behavior in this system. The in-chain superexchange coupling constant, as determined by a fit to the Bonner-Fisher model, is $|J|/k_B \approx 1300 \pm_{200}^{100}$ K, comparable to the values observed in the two-dimensional layered cuprates. Estimates of the interchain magnetic interaction indicate this material may be the best realization of a 1D spin- $\frac{1}{2}$ Heisenberg antiferromagnet reported to date. Low-temperature neutron and synchrotron x-ray powder-diffraction studies of Sr_2CuO_3 show that the low-temperature structure of this system has *Immm* space-group symmetry, the same structure reported at room temperature, indicating that this material, in contrast to La_2CuO_4 , does not undergo any structural transformations upon cooling. The absence of crystallographic distortions precludes a magnetic anisotropy contribution from a Dzyaloshinsky-Moriya interaction, implying that Sr_2CuO_3 should be a nearly ideal spin- $\frac{1}{2}$ antiferromagnetic Heisenberg chain compound, in agreement with the magnetic susceptibility results. A search for the presence of long-range three-dimensional antiferromagnetic order by magnetic neutron powder diffraction at temperatures as low as 1.5 K was not successful, although we estimate an upper limit for the size of the ordered moment which could have been detected to be $\sim 0.1\mu_B$ per Cu^{2+} ion.

INTRODUCTION

Since the discovery of high-temperature superconductivity, many studies have been performed both to search for new superconductors and elucidate the mechanism underlying the high transition temperatures (T_c). At this time, all known systems with $T_c > 40$ K possess two-dimensional CuO_2 sheets, which are generally agreed to play the active role in superconductivity. On the other hand, it has recently been reported¹ that $\text{Sr}_2\text{CuO}_{3+\delta}$ exhibits high-temperature superconductivity for appropriate values of δ . The parent insulating phase for these superconductors, Sr_2CuO_3 , has a crystal structure² in which one-dimensional Cu-O chains, similar to those in $\text{YBa}_2\text{Cu}_3\text{O}_7$, lie parallel to the *a* axis (Fig. 1). Although no one has reported superconductivity in materials that only have Cu-O one-dimensional chains, the observation of superconductivity in these materials raises important questions concerning the minimum magnetic and electronic dimensionalities, which will support high T_c . Furthermore, since the insulating parents of all other known high- T_c cuprate superconductors are two-dimensional spin- $\frac{1}{2}$ Heisenberg antiferromagnets,³ it is important to

understand the magnetism in this one-dimensional system as a prerequisite to determining its evolution as the system is doped into the metallic and superconducting state. Toward that end, we have studied the static magnetic properties of this material, and we observe direct evidence of Bonner-Fisher-type behavior,⁴ indicating that Sr_2CuO_3 is a nearly ideal one-dimensional (1D) spin- $\frac{1}{2}$ Heisenberg antiferromagnet.

EXPERIMENT

Sr_2CuO_3 was prepared by conventional solid-state reactions. Stoichiometric quantities of SrCO_3 and CuO were mixed and then calcined at 950°C under flowing oxygen (~ 1 l/min) for a total of 24 h with one intermediate grinding. The calcined powders were pulverized, pelletized, and sintered under the same conditions. Some samples were subjected to nitrogen treatment. Pellets were placed on an alumina boat and heated to between 400 and 1000°C under flowing nitrogen (~ 1 l/min) for 12 h. The decomposition temperature for this system is about 900°C under the nitrogen atmosphere we employed. This nitrogen gas is obtained from liquid-nitrogen boiloff and has a

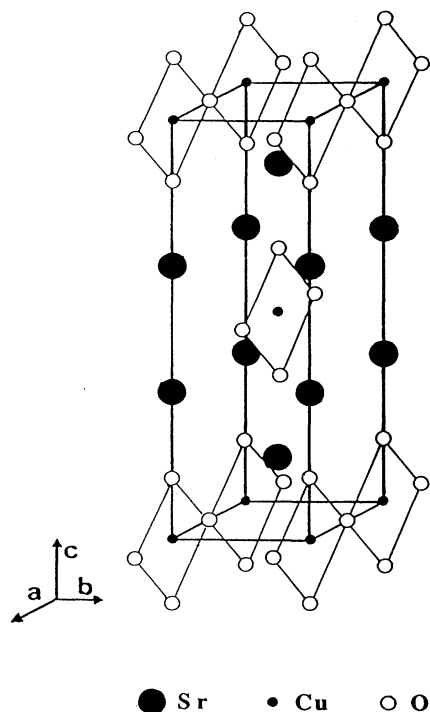


FIG. 1. The crystal structure of Sr_2CuO_3 . The Cu-O chains are parallel to the a axis. The apical oxygen is O(1) and the in-chain oxygen is O(2) in Table II.

small residual oxygen partial pressure. We expect that the decomposition temperature of Sr_2CuO_3 would decrease below 900°C if the oxygen partial pressure were further reduced and, in fact, samples heated above about 520°C in 6-Torr He do decompose. The oxygen contents of the samples were determined iodometrically.

Powder x-ray-diffraction data for initial characterization were obtained with a Scintag diffractometer using $\text{CuK}\alpha$ radiation at ambient temperature. Magnetic susceptibilities below 300 K were measured using a superconducting quantum interference device (SQUID) magnetometer (Quantum Design), whereas the high-temperature susceptibility (to 800 K) was measured using an Oxford Instruments Faraday balance. The contribution of ferromagnetic impurities to the measured magnetization was determined from magnetization-field isotherms between 25 and 750 K and was found to correspond to that of 2 at. ppm or less, with respect to Cu, of ferromagnetic iron metal impurities; this contribution is corrected for in Fig. 3 below. The magnetic measurements from the SQUID and the Faraday magnetometers were in good agreement below 300 K.

Low-temperature neutron powder-diffraction studies were carried out at 11 K using the BT-4 triple-axis spectrometer at the reactor facility of the National Institute of Standards and Technology. The collimation was $20'-40'-10'$, and the neutron wavelength (1.540 \AA) was chosen by a Cu (220) monochromator. The sample was mounted in an Al sample container containing He exchange gas. Low-temperature synchrotron x-ray

powder-diffraction⁵ data were collected at 12 K at beamline X-7A at the National Synchrotron Light Source at Brookhaven National Laboratory.

RESULTS

Magnetic susceptibility

There have been several previous studies⁶⁻⁸ of the magnetic susceptibility of Sr_2CuO_3 , but none of these studies observed clear evidence for Bonner-Fisher⁴ behavior, and therefore accurate values of J , the Cu^{2+} - Cu^{2+} nearest-neighbor superexchange coupling constant, were not determined. Furthermore, no systematic attempt was made in these earlier studies to account for the possible effect of oxygen nonstoichiometry on the magnetic susceptibilities. To address these problems, we have made magnetic susceptibility measurements over a wide range of temperatures on samples that have undergone various annealing treatments and therefore have slightly different oxygen contents (Table I). The susceptibility is strongly affected by such treatments. Figure 2 shows the temperature dependencies below 300 K of the magnetic susceptibilities of samples before and after annealing under a N_2 or a 6-Torr He atmosphere. The diamagnetic terms originating in the closed shells of the ions have been subtracted. ($\chi_{\text{dia}} = -77 \times 10^{-6} \text{ cm}^3/\text{mole}$). Plot (a) shows the susceptibility for an as-made sample before nitrogen treatment. As can be seen from this figure, treatment under a reducing atmosphere decreases the susceptibility, especially the Curie-type component. Thus it is natural to associate the magnitude of this Curie-type term with the presence of excess oxygen in the lattice. (This point will be discussed further below.) In this picture, the as-made sample (a) contains some excess oxygen-ion defects, whereas nitrogen annealing reduces the number of such defects and consequently suppresses the Curie-Weiss-like behavior at low temperatures. Furthermore, Fig. 2 shows the susceptibility for a sample that was kept at 600 K under 6-Torr He overnight and then measured *without* being removed from the He atmosphere. This sample shows a much smaller Curie-Weiss-type term compared with the other samples, presumably due to loss of almost all the excess oxygen after the overnight anneal. Since samples annealed in N_2 , but then exposed to air before the magnetic measurements were

TABLE I. Parameters for $\text{Sr}_2\text{CuO}_{3+\delta}$ derived from iodometric titrations and magnetic refinements assuming that $g=2.1$, $|J|/k_B=1307 \text{ K}$.

Samples (conditions)	Oxygen content (δ)	Spin- $\frac{1}{2}$ impurity level (%)	θ (K)	Van Vleck susceptibility (cm^3/mole)
(a) 950°C in O_2	0.02(2)	0.363	-1.09	2.87×10^{-5}
(b) 600°C in N_2	0.01(1)	0.287	-0.83	2.91×10^{-5}
(c) 800°C in N_2	-0.01(1)	0.227	-0.86	2.63×10^{-5}
(d) 327°C in 6-Torr He	No data	0.114	-7.81	2.28×10^{-5}

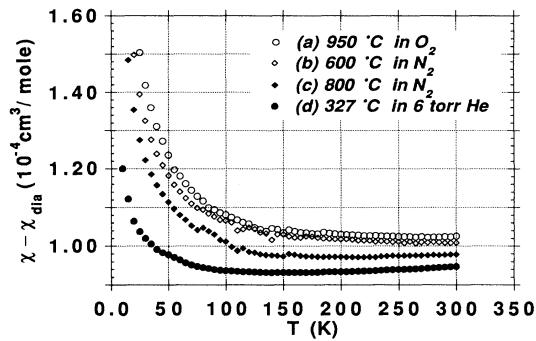


FIG. 2. The temperature (T) dependencies of the magnetic susceptibility (χ) for samples before and after annealing under atmospheres of nitrogen or 6-Torr He. The diamagnetic core contributions (χ_{dia}) have been subtracted. The measurement magnetic field was 1.0 T.

made, have larger Curie-Weiss-type terms, we suggest that this material absorbs oxygen from air at room temperature fairly quickly, and that considerable care must be taken if one wishes to measure properties for the stoichiometric system.

Figure 3 shows the susceptibility versus temperature from 10 to 800 K for the sample annealed at 327°C (600 K) under 6-Torr He and then measured in the same atmosphere. Between 25 and 750 K the susceptibility was found to be independent of applied magnetic field H up to $H=7.0$ T (after correction for the influence of ferromagnetic impurities; see above). The enhancement of the susceptibility at low temperature presumably originates from a residual Curie-Weiss-like component, as mentioned above, but the gradual increase of the susceptibility with increasing temperature in the high-temperature region is not Curie-Weiss-like, but rather is similar to a Bonner-Fisher-type susceptibility,⁴ as our fit to the data described below demonstrates.

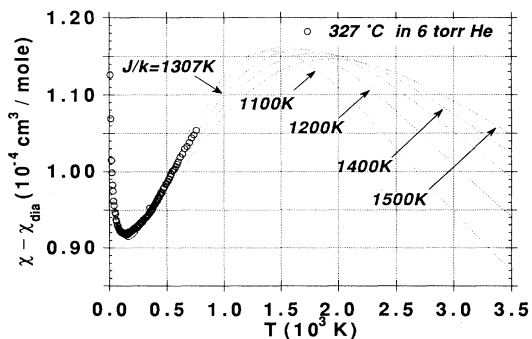


FIG. 3. The magnetic susceptibility ($\chi - \chi_{\text{dia}}$) vs temperature up to 800 K for the sample measured under 6-Torr helium. The experimental data are represented by open circles, while the theoretical curves described in the text are shown by dotted lines.

Synchrotron- and neutron-diffraction studies

The crystal structure of Sr_2CuO_3 at room temperature was first determined by single-crystal x-ray diffraction.² Powder neutron⁹ and x-ray-diffraction¹⁰ data at room temperature have also been reported. All of these studies assigned the orthorhombic $Immm$ space group to Sr_2CuO_3 . We utilized neutron and synchrotron x-ray powder diffraction at low temperatures in order to search for any evidence of structural phase transitions or distortions, which would further lower the symmetry and, for example, contribute to the magnetic anisotropy by allowing a Dzyaloshinsky-Moriya (DM) interaction¹¹ to occur. It is known that the leading-order magnetic anisotropy in several of the cuprates, for example, La_2CuO_4 , arises from the DM interaction.

Structural information determined by Rietveld refinement¹² of neutron-diffraction data (Fig. 4) obtained at 11 K are shown in Table II. Aluminum reflections from the sample container used were excluded from the refinement. No superlattice peaks, which would indicate lattice distortion, were observed. High-resolution synchrotron x-ray-diffraction data (Fig. 5) at 12 K yielded a similar conclusion. These results show that there are no structural transformations in Sr_2CuO_3 between room temperature and 11–12 K.

We also note that recent muon spin rotation data⁸ have been interpreted as offering evidence for three-dimensional magnetic ordering in Sr_2CuO_3 (synthesized in air) with a Néel temperature of 5 K. Since we observed no magnetic neutron powder diffraction at 1.5 K for a similar sample prepared in air, we conclude either that the Néel temperatures are different for these two samples, that only short-range magnetic ordering occurs, or that the ordered moment is simply too small to be observed by neutron powder diffraction. In fact, we have estimated an upper limit for the magnitude of the Cu^{2+} magnetic moment, which would have been observable in our neutron-diffraction measurements, if these moments exhibited long-range 3D antiferromagnetic order characterized by an antiferromagnetic propagation vector and spin direction similar to those observed for other

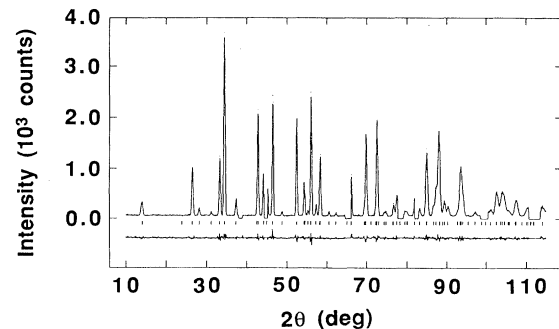


FIG. 4. Powder neutron-diffraction data collected at 11 K. The results of Rietveld refinement are superimposed on the raw data. The vertical tick marks indicate the expected location of diffraction peaks. The fit residuals are plotted at the bottom of the figure. The neutron wavelength was 1.5401 Å.

TABLE II. Low-temperature crystallographic data for Sr_2CuO_3 determined by Rietveld refinement of neutron-diffraction data obtained at 11 K.

Space group: $Im\bar{m}m$; Lattice constants: $a=3.9089(2) \text{ \AA}$ $b=3.4940(2) \text{ \AA}$ $c=12.6910(7) \text{ \AA}$ $V=173.33(3) \text{ \AA}^3$						
Atom	Position (site symmetry)	x	y	z	$U_{\text{iso}} (\text{\AA}^2)$	Occupancy
Sr	$4i$ ($mm2$)	0	0	0.35195(9)	0.006(4)	0.980(4)
Cu	$2a$ (mmm)	0	0	0	0.001(5)	0.990(6)
O(1)	$4i$ ($mm2$)	0	0	0.15445(11)	0.0027(5)	1.000(5)
O(2)	$2b$ (mmm)	0.5	0	0	0.0021(8)	0.993(8)
$R_p(\%)=6.03$		$R_{\text{wp}}(\%)=8.91$		$R_e(\%)=6.84$		$R_f(\%)=2.04$
Selected bond distances (\AA) for Sr_2CuO_3 at 11 K						
Cu-O(1)	1.9601(15) \AA					
Cu-O(2)	1.9545(1) \AA					
Sr-O(1)	2.5065(27) \AA					

K_2NiF_4 -type oxides such as La_2CuO_4 (Ref. 13), La_2NiO_4 (Ref. 14), or Ca_2MnO_4 (Ref. 15). For example, if the antiferromagnetic ordering was such that the $(\frac{1}{2}, \frac{1}{2}, 1)$ were an allowed magnetic Bragg reflection, then an ordered moment $\geq 0.1 \mu_B$ would have yielded an observable peak intensity. The same is approximately true for other magnetic peaks with (hkl) values corresponding to $0.7 \text{ \AA}^{-1} \leq Q \leq 2.0 \text{ \AA}^{-1}$. Thus, our sample either did not exhibit long-range magnetic order, or the size of the ordered moment is less than $0.1 \mu_B$. The latter situation could arise due to strong renormalization of the ordered moment as a result of quantum fluctuations. Quantum fluctuations are generally more important in 1D than in

2D magnetic systems and are particularly large for spin- $\frac{1}{2}$ ions such as Cu^{2+} . Table III lists classical and observed values for the ordered moments for several 1D antiferromagnets,¹⁶⁻¹⁷ clearly demonstrating the moment renormalization due to quantum fluctuations. It is also obvious from these data that the effect of fluctuations indeed grows as the value of the spin decreases, and might therefore be expected to reduce the ordered moment by more than a factor of 2 in a spin- $\frac{1}{2}$ material such as Sr_2CuO_3 . Experimental resolution of this issue must

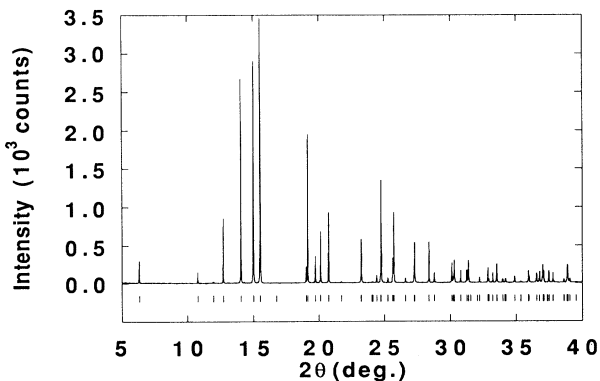


FIG. 5. Synchrotron x-ray-diffraction data collected at 12 K. The vertical tick marks indicate the expected location of diffraction peaks. The x-ray wavelength was 0.70377 \AA .

TABLE III. Renormalization of ordered magnetic moment due to quantum fluctuations for several materials. Classical moments were calculated assuming all gyromagnetic factors $g=2$. The ratios of the measured to the classical ordered moments are listed in the second to last column.

Ion	Compound	Classical ordered moment (μ_B)	Measured ordered moment (μ_B)	Ratio
Cu^{2+} ($S=1/2$)	KCuF_3^a	1	0.49	0.49
Ni^{2+} ($S=1$)	CsNiCl_3^b	2	1.05	0.525
Ni^{2+} ($S=1$)	RbNiCl_3^b	2	1.3	0.65
Mn^{2+} ($S=5/2$)	CsMnBr_3^b	5	3.5	0.70
Mn^{2+} ($S=5/2$)	RbMnBr_3^b	5	3.6	0.72

^aReference 16.

^bReference 17.

await systematic results for single crystals with well-controlled oxygen contents.

DISCUSSION

The magnetic Hamiltonian, which describes a spin- $\frac{1}{2}$ Heisenberg chain,

$$H = 2|J| \sum_i \mathbf{S}_i \cdot \mathbf{S}_{i+1}, \quad (1)$$

was described previously.⁴ In this expression, J is the Cu^{2+} - Cu^{2+} intrachain superexchange coupling constant, and the summation extends over pairs of nearest-neighbor spins. It is worthwhile spending a moment to justify the use of such a model to describe the magnetic susceptibility of Sr_2CuO_3 . The assumption that Sr_2CuO_3 is a one-dimensional magnetic system follows directly from the structure of this material (Fig. 1). Since the Cu^{2+} ions are only bonded to oxygen ions along the a direction with 180° Cu—O—Cu bonds, there will be strong Cu^{2+} - Cu^{2+} antiferromagnetic superexchange interactions only in this direction. The additional assumption that this is a Heisenberg system is based upon the fact that the Cu^{2+} ion is spin $\frac{1}{2}$ and thus has no single-ion anisotropy to first order. Furthermore, the structural studies reported here and previously^{9,10} for Sr_2CuO_3 demonstrate that there is an inversion center located midway between the Cu^{2+} ions in the Cu-O chains, which precludes the existence of a Dzyaloshinsky-Moriya (DM) $\mathbf{S}_i \times \mathbf{S}_j$ interaction.¹¹ In contrast, La_2CuO_4 , an antiferromagnetic insulator, which is structurally similar to Sr_2CuO_3 , has a leading-order magnetic anisotropy arising from a DM interaction, which is allowed by the rotational distortion of the CuO_6 octahedra in the $Bmab$ (orthorhombic) phase.¹⁸ We also expect that the interchain magnetic coupling will be rather weak in this material, partly as a result of magnetic frustration. For example, the *interlayer* interchain superexchange in Sr_2CuO_3 is fully frustrated *despite* the orthorhombic symmetry, again in contrast to the situation in orthorhombic La_2CuO_4 , where the *interlayer* superexchange is not frustrated. This is true because, considering a given Cu^{2+} ion, the four nearest-neighbor Cu^{2+} ions in the nearest-neighbor chains in adjacent layers are *equidistant* in Sr_2CuO_3 , whereas in La_2CuO_4 there are *two* such distances. The *intralayer* interchain interaction is, on the other hand, not frustrated, but is still expected to be rather weak due to the absence of intervening oxygen ions between adjacent Cu^{2+} ions. Thus, in general, one expects Sr_2CuO_3 to be more Heisenberg-like than La_2CuO_4 , the latter nevertheless being considered one of the best examples of a spin- $\frac{1}{2}$ 2D Heisenberg antiferromagnet.¹⁹ Therefore, we should expect Sr_2CuO_3 to be an excellent realization of a 1D Heisenberg antiferromagnet, and it seems very reasonable to attempt to describe its magnetic susceptibility with the Bonner-Fisher model for a spin- $\frac{1}{2}$ Heisenberg antiferromagnetic chain.

In order to fit the susceptibility data shown in Fig. 3 over a wide temperature range, we assume that the ob-

served temperature-dependent magnetic susceptibility, $\chi(T)$, consists of three terms:

$$\chi(T) = \chi_{\text{dia}} + \chi_{\text{VV}} + \chi_{\text{spin}}(T), \quad (2)$$

where χ_{dia} is due to the diamagnetism of the core electron shells, χ_{VV} is the Van Vleck paramagnetism of the open shells of the Cu^{2+} ions, and $\chi_{\text{spin}}(T)$ is the Cu^{2+} spin susceptibility. In the absence of appreciable numbers of conduction electrons, the Pauli paramagnetism and the Landau diamagnetism should be negligible. χ_{dia} and χ_{VV} are assumed to be temperature independent, and the values of χ_{dia} used were found in Ref. 20. Furthermore, the spin susceptibility was separated into two parts:

$$\chi_{\text{spin}}(T) = \rho(\chi_{\text{CW}}) + (1 - \rho)\chi_{\text{BF}} \quad (3)$$

where χ_{CW} is a Curie-Weiss-like component arising from finite length chains, which consist of an odd number of Cu^{2+} spins,⁴ isolated Cu^{2+} spins, and/or other paramagnetic impurities, and χ_{BF} is the susceptibility of an $S = \frac{1}{2}$ infinite isotropic Heisenberg chain (the Bonner-Fisher susceptibility^{4,21}). The coefficient ρ represents the defect and/or impurity level. There are no analytical solutions for the magnetic susceptibility of Heisenberg chains.⁴ However, a useful closed-form approximation to χ_{BF} has been suggested²² to be

$$\chi_{\text{BF}} = \frac{Ng^2\mu_B^2}{k_B T} \left[\frac{0.25 + 0.14995x + 0.30094x^2}{1 + 1.9862x + 0.68854x^2 + 6.0626x^3} \right] \quad (4)$$

with $x = |J|/k_B T$. The Curie-Weiss-like term is

$$\chi_{\text{CW}} = \frac{Ng^2\mu_B^2 S(S+1)}{3k_B(T-\theta)}. \quad (5)$$

Assuming that $g = 2.1$, a typical value for cuprates,^{3,23} and $S = \frac{1}{2}$, we determine the following parameters by fitting Eq. (2) to the magnetic susceptibility data in Fig. 3 after subtracting the core diamagnetism:

$$\rho = 1.14 \times 10^{-3} \text{ (i.e., impurity level = 0.11\%)},$$

$$\theta = -7.81 \text{ K},$$

$$|J|/k_B = 1307 \text{ K},$$

$$\chi_{\text{VV}} = 2.28 \times 10^{-5} \text{ cm}^3/\text{mole}.$$

The value of χ_{VV} is comparable to that of other single Cu-O layer cuprates.²⁴ The fit using these parameter values is shown superimposed on the data in Fig. 3. The fit function has been extended to temperatures high enough to include the broad peak in the susceptibility arising from the appearance of short-range 1D order with decreasing temperature. Furthermore, several curves calculated assuming different values of J are plotted to give a sense of the sensitivity of the fit to this important parameter. From these curves we estimate the value of $|J|/k_B$ to be 1300_{-200}^{+100} K.

As mentioned previously, a Curie-Weiss-type term can originate from several possible sources, including nearly isolated Cu^{2+} ions associated with oxygen defects (oxy-

gen vacancies or excess oxygen), some other kind of lattice defect, or magnetic impurities. However, an equally plausible explanation is that the Curie-like behavior originates from Cu-O 1D chains, which are randomly terminated by oxygen defects. As Bonner and Fisher have discussed,⁴ if the resulting chains have an even number of Cu²⁺ spins, then the total spin on the chain in the antiferromagnetically ordered state is zero at $T=0$. If, however, the chains have an odd number of Cu²⁺ spins, then in the antiferromagnetically ordered state the net spin on the chain is $\frac{1}{2}$. Such chains of odd length will make contributions to the magnetic susceptibility, which are Curie-Weiss-like, although both the amplitude of the susceptibility divergence and the temperature at which the divergence occurs are depressed with increasing chain length by Cu²⁺-Cu²⁺ antiferromagnetic interactions. In the opposite limit, "chains" that have a length of only one Cu²⁺ will precisely exhibit Curie-Weiss behavior. To avoid the additional complications necessary to model contributions to the magnetic susceptibility arising from chains with a random distribution of lengths, we have chosen to represent the spin susceptibility for Sr₂CuO₃ simply as a Curie-Weiss term plus a Bonner-Fisher term. We thus assume that the inclusion of a Curie-Weiss term will adequately represent the contributions from odd length finite chains, as well as additional contributions due to isolated Cu²⁺ ions and/or impurities. This simplification minimizes the number of refinement parameters, and the quality of the fit indicates it to be a reasonable approximation.

The results of these measurements thus indicate that Sr₂CuO₃ is an excellent realization of a 1D spin- $\frac{1}{2}$ Heisenberg antiferromagnet. In fact, it may be the best realiza-

tion of such a system reported to date. In order to place Sr₂CuO₃ in the context of other 1D antiferromagnets, Table IV shows parameters for several such systems, which have appeared in the literature.¹⁷ J_1 and J_2 are the two interchain magnetic coupling constants in orthogonal directions (in the b and c directions in Sr₂CuO₃). For all materials^{16,17,25,26} other than Sr₂CuO₃ in Table IV we have assumed that $J_1=J_2$. We have also calculated independent values of J_1 and J_2 for Sr₂CuO₃, assuming only dipolar interchain coupling, using the expression

$$J_\alpha = - \sum_i \frac{\mu \cdot \mu_i (3 \cos^2 \phi_i - 1)}{r_i^3}, \quad (6)$$

where the sum is over the Cu moments μ_i in the same ($J_\alpha=J_1$) or different ($J_\alpha=J_2$) layers, r_i is the vector from the moment μ to the moment μ_i , and ϕ_i is the angle between r_i and the a axis. For this calculation the magnetic structure was assumed to be the same as that reported for Sr₂CuO₂Cl₂ (Ref. 27): in our case we assume the Cu²⁺ spins to be either parallel or antiparallel to the a axis. The summation in Eq. (6) included Cu²⁺ moments within a distance r_i sufficient to achieve convergence.

Values of J_1 ($=J_2$) in Table IV were calculated from the following expressions²⁸⁻³⁰ using experimental values^{8,17} of T_N and J :

$$\frac{kT_N}{|J|} = \frac{4S(S+1)/3}{I(\eta_1, \eta_2)}, \quad (7)$$

where $\eta_1=J_1/J$, $\eta_2=J_2/J$, and

TABLE IV. J , J_1 , J_2 , and T_N values for several linear chain antiferromagnets compared with the values for Sr₂CuO₃. Note that J_1 and J_2 for Sr₂CuO₃ are the values estimated assuming only dipolar coupling between the Cu²⁺ spins. For the other cases, η_1 ($=\eta_2$) and J_1 ($=J_2$) are estimated from the experimental Néel temperatures. The experimental value of 5 K for the Néel temperature of Sr₂CuO₃ was taken from Ref. 8 (other data from Refs. 16 or 17 unless otherwise noted); the much smaller value of 0.028 K is estimated from expressions (7)–(9) given in the text assuming that the only source of interchain coupling (J_1 and J_2) is the magnetic dipole interaction given by Eq. (6).

	T_N (K)	J (K)	S (spin)	$I(\eta_1, \eta_2)$	η_1	η_2	J_1 (K)	J_2 (K)
Sr ₂ CuO ₃	0.028 ^a	1307	1/2	4.7×10^4	2.8×10^{-5}	5.1×10^{-7}	0.036	6.6×10^{-4}
	5 ^b	1307	1/2	260	6.06×10^{-6}			7.88×10^{-3}
TMMC ^c	0.84	6.5	5/2	90.3	5.03×10^{-5}			3.27×10^{-4}
RbMnBr ₃ ^d	8.8	12	5/2	15.9	1.62×10^{-3}			1.94×10^{-2}
CsMnBr ₃ ^d	8.3	9.6	5/2	13.5	2.25×10^{-3}			2.16×10^{-2}
CuCl ₂ ·2NC ₃ H ₅	1.7	13	1/2	7.65	7.00×10^{-3}			9.10×10^{-2}
CsNiCl ₃	4.5	11	1.0	6.52	9.64×10^{-3}			0.106
KCuF ₃	39.8	203	1/2	6.40	1.4×10^{-2e}			3.2 ^e
					1.0×10^{-2f}			1.90 ^f
RbNiCl ₃	11	11	1.0	2.67	5.76×10^{-2}			0.634

^aValue calculated assuming dipolar coupling only.

^bValue quoted from Ref. 8 (μ SR data).

^c(CH₃)₄NMnCl₃.

^d J , T_N , and S from Ref. 25.

^eEstimated from Eqs. (7) and (9).

^fNeutron scattering results (from spin-wave dispersion perpendicular to chain direction) from Ref. 26.

$$I(\eta_1, \eta_2) = \frac{1}{\pi^3} \int \int \int_0^\pi \frac{dq_x dq_y dq_z}{\eta_1(1 - \cos q_x) + \eta_2(1 - \cos q_y) + (1 - \cos q_z)}. \quad (8)$$

For the case, where $J/J_1 \gg 1$, and $J_1/J_2 \geq 1$, Eq. (8) can be approximated by³⁰

$$I(\eta_1, \eta_2) = \frac{0.64}{\sqrt{\eta_1}} \left[1 + 0.253 \ln \left(\frac{\eta_1}{\eta_2} \right) \right]. \quad (9)$$

For $J/J_1 \geq 10$, we find that Eq. (9) is accurate to better than 5%. Thus the interchain coupling energies can be estimated using the experimental values of T_N and J in Eqs. (7) and (9).

The fact that we observe no evidence for 3D magnetic order in our samples above $T=2$ K would be consistent with the value of $T_N=0.028$ K from Eq. (7), calculated assuming only interchain dipolar magnetic coupling (Table IV). The much larger value of $T_N=5$ K reported in Ref. 8 would thus imply that there is interchain coupling, in addition to that due to the magnetic dipole interaction, in Sr_2CuO_3 (see Table IV). Additional measurements, including magnetic susceptibility, specific heat and neutron diffraction, to temperatures lower than 2K would be of great interest in the study of 3D magnetic order in this system.

We note here that any long-range three-dimensional antiferromagnetic structure adopted by Sr_2CuO_3 must be one in which the Cu^{2+} moments order antiferromagnetically within each chain; that is, a ferromagnetic intrachain interaction with an antiferromagnetic interchain interaction would not be consistent with our magnetic susceptibility data. Our low-temperature structural data provide evidence that the magnetic properties of this material are not influenced by complications such as structural phase transformations or stabilization of a spin Peierls state, as occurs in CuGeO_3 (Ref. 31). A number of other spin- $\frac{1}{2}$ Heisenberg chains based upon Cu^{2+} have also been reported,^{16,17,24} but all of these compounds have values of J much smaller than Sr_2CuO_3 . The value we measure here, $|J|/k_B \approx 1300$ K, is quite large and comparable to that measured in the 2D cuprate systems. It should be pointed out here that in the layered cuprate literature the prefactor of the sum over nearest-neighbor pairs in the Hamiltonian of Eq. (1) has the factor of 2 missing. Thus one should compare $2J$ (2600 K) for Sr_2CuO_3 with J (~ 1500 K) in the layered cuprate literature. It is an open question why the nearest-neighbor Cu-Cu superexchange interaction in Sr_2CuO_3 is significantly larger than in the antiferromagnetic layered cuprate systems.

Finally, the evolution of the magnetic and electronic dimensionalities in $\text{Sr}_2\text{CuO}_{3+\delta}$ as a function of δ is a very important subject for future study. Although there are apparently several superconducting phases^{1,32,33} in this system, their crystal structures, particularly the precise oxygen ordering arrangements, have yet to be determined. Thus the intriguing question of how a 1D antiferromagnet evolves into a high-temperature superconductor in this system remains to be answered.

CONCLUSION

Magnetic susceptibility measurements for Sr_2CuO_3 indicate that this system is a nearly ideal spin- $\frac{1}{2}$ Heisenberg antiferromagnetic chain with an in-chain superexchange coupling constant of $|J|/k_B \approx 1300_{-200}^{+100}$ K. The ratio of the interchain to intrachain magnetic coupling is smaller than any values previously reported for one-dimensional antiferromagnets. The crystal structure of Sr_2CuO_3 , as determined by neutron and synchrotron x-ray diffraction, does not undergo any lattice distortion between room temperature and 11 K, indicating that any magnetic anisotropy should be weak. The good agreement of the magnetic susceptibility data with the predictions of the Bonner-Fisher model for a spin- $\frac{1}{2}$ antiferromagnetic Heisenberg chain are consistent with this expectation. Finally, no evidence for long-range antiferromagnetic order was observed above 2 K.

ACKNOWLEDGMENTS

The authors thank A. Keren and Y. J. Uemura (Columbia University) and G. Shirane (Brookhaven National Laboratory) for helpful discussions, N. Herron (DuPont) for iodometric titrations, D. E. Cox (Brookhaven National Laboratory) for help with the synchrotron x-ray-diffraction measurements, and S. Pace (Iowa State University) for assistance with numerical integration of Eq. (8). The work at the National Synchrotron Light Source, Brookhaven National Laboratory was supported by the U. S. Department of Energy, Division of Materials Sciences and Division of Chemical Sciences. Ames Laboratory is operated for the U. S. Department of Energy by Iowa State University under Contract No. W-7405-Eng-82. The work at Ames was supported by the Director for Energy Research, Office of Basic Energy Sciences.

*Permanent Address: Sony Research Center, 174, Fujitsuka-cho, Hodogaya-ku, Yokohama, 240 Japan.

¹Z. Hiroi, M. Takano, M. Azuma, and Y. Takeda, *Nature* (London) **364**, 315 (1993).

²Chr. L. Teske and Hk. Muller-Büschbaum, *Z. Anorg. Allg.*

Chem. **371**, 325 (1969).

³For example, see D. C. Johnston, *J. Magn. Magn. Mater.* **100**, 218 (1991).

⁴J. C. Bonner and M. E. Fisher, *Phys. Rev.* **135**, A640 (1964).

⁵The diffractometer was operated in the high-resolution mode

- described by D. E. Cox, B. H. Toby, and M. M. Eddy, *Aust. J. Phys.* **41**, 117 (1988).
- ⁶Y. J. Shin, E. D. Manova, J. M. Dance, P. Dordor, J. C. Grenier, E. Marquestaut, J. P. Doumerc, M. Pouchard, and P. Hagenmuller, *Z. Anorg. Allg. Chem.* **616**, 201 (1992).
- ⁷S. Kondoh, K. Fukuda, and M. Sato, *Solid State Commun.* **65**, 1163 (1988).
- ⁸A. Keren, L. P. Le, G. M. Luke, B. J. Sternlieb, W. D. Wu, Y. J. Uemura, S. Tajima, and S. Uchida, *Phys. Rev. B* **48**, 12 926 (1993).
- ⁹M. T. Weller and D. R. Lines, *J. Solid State Chem.* **82**, 21 (1989).
- ¹⁰Ch. Kruger, W. Reichelt, A. Almes, U. Konig, H. Oppermann, and H. Scheler, *J. Solid State Chem.* **96**, 67 (1992); D. R. Lines, M. T. Weller, D. B. Currie, and D. M. Osborne, *Mater. Res. Bull.* **26**, 323 (1991).
- ¹¹I. Dzyaloshinsky, *J. Phys. Chem. Solids* **4**, 241 (1958); T. Moriya, *Phys. Rev.* **120**, 91 (1960); T. Moriya, in *Magnetism*, edited by G. T. Rado and H. Suhl (Academic, New York, 1963), Vol. I, Chap. 3.
- ¹²Structural refinements were made using the GSAS software package [A. C. Larsen and R. B. von Dreele, LANSCE, Los Alamos National Laboratory (1990)].
- ¹³D. Vaknin, S. K. Sinha, D. E. Moncton, D. C. Johnston, J. M. Newsam, C. R. Safinya, and H. E. King, Jr., *Phys. Rev. Lett.* **58**, 2802 (1987); B. X. Yang, S. Mitsuda, G. Shirane, Y. Yamaguchi, H. Yamauchi, and Y. Syono, *J. Phys. Soc. Jpn.* **56**, 2283 (1987).
- ¹⁴G. Aeppli and D. J. Buttrey, *Phys. Rev. Lett.* **61**, 203 (1988).
- ¹⁵D. E. Cox, G. Shirane, R. J. Birgeneau, and J. B. MacChesney, *Phys. Rev.* **188**, 930 (1969).
- ¹⁶M. T. Hutchings, E. J. Samuelsen, G. Shirane, and K. Hirakawa, *Phys. Rev.* **188**, 919 (1969).
- ¹⁷L. J. De Jongh and A. R. Miedema, *Adv. Phys.* **23**, 1 (1974); M. Steiner, J. Villain, and C. G. Windsor, *ibid.* **25**, 87 (1976).
- ¹⁸T. Thio, T. R. Thurston, N. W. Preyer, P. J. Picone, M. A. Kastner, H. P. Jensen, D. R. Gabbe, M. Sato, K. Fukuda, S. Shamoto, Y. Endoh, K. Yamada, and G. Shirane, *Phys. Rev. B* **38**, 905 (1988).
- ¹⁹R. J. Birgeneau and G. Shirane, in *Physical Properties of High Temperature Superconductors I*, edited by D. M. Ginsberg (World Scientific, New Jersey, 1989), Chap. 3.
- ²⁰E. A. Boudreaux and L. N. Mulay, *Theory and Applications of Molecular Paramagnetism* (Wiley, New York, 1976), p. 494.
- ²¹R. L. Carlin, *Magnetochemistry* (Springer-Verlag, Berlin, 1986).
- ²²W. E. Estes, D. P. Gavel, W. E. Hatfield, and D. J. Godjson, *Inorg. Chem.* **17**, 1415 (1978).
- ²³H. Ohta, N. Yamauchi, M. Motokawa, M. Azuma, and M. Takano, *J. Phys. Soc. Jpn.* **61**, 3370 (1992).
- ²⁴C. Allgeier and J. S. Schilling, *Phys. Rev. B* **48**, 9747 (1993).
- ²⁵C. J. Glinka, V. J. Minkiewicz, D. E. Cox, and C. P. Khatak, in *Magnetism and Magnetic Materials*, edited by C. D. Graham and J. J. Rhyne, AIP Conf. Proc. 10 (AIP, New York, 1972), p. 659; M. Eibschutz, R. C. Sterwood, F. S. L. Hsu, and D. E. Cox, *ibid.*, p. 684.
- ²⁶S. K. Satija, J. D. Axe, G. Shirane, H. Yoshizawa, and K. Hirakawa, *Phys. Rev. B* **21**, 2001 (1980).
- ²⁷D. Vaknin, S. K. Sinha, C. Stassis, L. L. Miller, and D. C. Johnston, *Phys. Rev. B* **41**, 1926 (1990).
- ²⁸T. Oguchi, *Phys. Rev.* **133**, A1098 (1964).
- ²⁹E. Montroll, *Proceedings of the Third Berkeley Symposium on Mathematical Statistics and Probability, Berkeley, CA, 1955*, edited by Jerzy Neyman (University of California Press, Berkeley, 1956), Vol. 3.
- ³⁰M. J. Hennessy, C. D. McElwee, and P. M. Richards, *Phys. Rev. B* **7**, 930 (1973).
- ³¹M. Hase, I. Terasaki, and K. Uchinokura, *Phys. Rev. Lett.* **70**, 3651 (1993).
- ³²P. Laffez, S. Adachi, H. Yamauchi, and N. Mori, *Proceedings of the International Conference on "Superconducting Materials," Paris, 1993 (ICMAS-93)*, edited by J. Etourneau, J. B. Torrance, and H. Yamauchi (IITT International, Paris, 1993).
- ³³T. Ami and M. K. Crawford (unpublished data).